American Society of Hematology
2021 L Street NW, Suite 900,
Washington, DC 20036
Phone: 202-776-0544 | Fax 202-776-0545
editorial@hematology.org

EBF1 and PAX5 control pro-B cell expansion via opposing regulation of the *Myc* gene.

Tracking no: BLD-2020-009564R1

Rajesh Somasundaram (Linkoping univesity, Sweden) Christina Jensen (Laboratory Medicine, Sweden) Johanna Tingvall-Gustafsson (Lund University, Sweden) josefine åhsberg (Linköping University, Sweden) Kazuki Okuyama (Linköping University, Sweden) Mahadesh Prasad (Linkoping univesity, Sweden) James Hagman (National Jewish Health, United States) Xun Wang (Caltech, United States) Shamit Soneji (Lund University, Sweden) Tobias Strid (Linkoping univesity, Sweden) Jonas Ungerbäck (Lund University, Sweden) Mikael Sigvardsson (Lund University, Sweden)

Abstract:
Genes encoding B lineage restricted transcription factors are frequently mutated in B-lymphoid leukemias, suggesting a close link between normal and malignant B-cell development. One of these transcription factors is Early B cell Factor 1 (EBF1), a protein of critical importance for lineage specification and survival of B-lymphoid progenitors. Here, we report that impaired EBF1 function in mouse B-cell progenitors results in reduced expression of *Myc*. Ectopic expression of MYC partially rescued B-cell expansion in the absence of EBF1 both *in vivo* and *in vitro*. Using chromosome conformation analysis in combination with ATAC-seq, ChIP-seq and reporter gene assays, we identified six EBF responsive enhancer elements within the *Myc* locus. CRISPR-Cas9 mediated targeting of EBF1 binding sites identified one element of key importance for *Myc* expression and pro-B cell expansion. These data provide evidence that *Myc* is a direct target of EBF1. Furthermore, ChIP-seq analysis revealed that several regulatory elements in the *Myc* locus are targets of PAX5. However, ectopic expression of PAX5 in EBF1 deficient cells inhibits the cell cycle and reduces *Myc* expression, suggesting that EBF1 and PAX5 act in an opposing manner to regulate *Myc* levels. This hypothesis is further substantiated by the finding that *Pax5* inactivation reduces requirements for EBF1 in pro-B cell expansion. The binding of EBF1 and PAX5 to regulatory elements in the human *MYC* gene in a B-ALL cell line indicate that the *EBF1:PAX5:MYC* regulatory loop is conserved and may control both normal and malignant B-cell development.

Conflict of interest: No COI declared

COI notes:

Preprint server: No;

Author contributions and disclosures: KO, TS, RS, CJ, JTG, MP, JÅ, MS and JU designed conducted and analyzed experiments. SS, JU, CJ and TS contributed to the bioinformatic analysis. JRH and XW contributed essential reagents and analyzed data. MS designed experiments analyzed data and wrote the manuscript draft. All authors contributed to the final version of the manuscript.

Non-author contributions and disclosures: No;

Agreement to Share Publication-Related Data and Data Sharing Statement: Sequencing data is deposited in GEO as: GSE136238 (Figure 1 and S1) and GSE159957 (Figure 3, 5).

Clinical trial registration information (if any):

EBF1 and PAX5 control pro-B cell expansion via opposing regulation of the *Myc* gene.

Rajesh Somasundaram[1,€], Christina T Jensen[5,€], Johanna Tingvall-Gustafsson[5] , Josefine Åhsberg[1], Kazuki Okuyama[1], Mahadesh Prasad[1], James R. Hagman[3,4], Xun Wang[2], Shamit Soneji[5], Tobias Strid[1] , Jonas Ungerback[5] and Mikael Sigvardsson[1,5,*]

1 Department of Biomedical and Clinical Sciences, Linköping University, Sweden.

2 Division of Biology & Biological Engineering, California Institute of Technology, Pasadena, CA 91125, USA;

3 Department of Immunology and Genomic Medicine, National Jewish Health, Denver, CO 80206, USA.

4 Department of Immunology and Microbiology, University of Colorado Anschutz Medical Campus, Aurora, CO 80045, USA.

5 Division of Molecular Hematology, Lund University, Lund, Sweden

€ Equal contribution

*Corresponding author: Mikael Sigvardsson, Division of Molecular Hematology, BMC B12, 22184 Lund, Sweden. E-mail: mikael.sigvardsson@med.lu.seTel: 46-708-320120

Running title: Opposing regulation of Myc by EBF1 and PAX5.

Word count: 4000

Abstract:

Genes encoding B lineage restricted transcription factors are frequently mutated in B-lymphoid leukemias, suggesting a close link between normal and malignant B-cell development. One of these transcription factors is Early B cell Factor 1 (EBF1), a protein of critical importance for lineage specification and survival of B-lymphoid progenitors. Here, we report that impaired EBF1 function in mouse B-cell progenitors results in reduced expression of *Myc*. Ectopic expression of MYC partially rescued B-cell expansion in the absence of EBF1 both *in vivo* and *in vitro.* Using chromosome conformation analysis in combination with ATAC-seq, ChIP-seq and reporter gene assays, we identified six EBF responsive enhancer elements within the *Myc* locus. CRISPR-Cas9 mediated targeting of EBF1 binding sites identified one element of key importance for *Myc* expression and pro-B cell expansion. These data provide evidence that *Myc* is a direct target of EBF1. Furthermore, ChIP-seq analysis revealed that several regulatory elements in the *Myc* locus are targets of PAX5. However, ectopic expression of PAX5 in EBF1 deficient cells inhibits the cell cycle and reduces *Myc* expression, suggesting that EBF1 and PAX5 act in an opposing manner to regulate *Myc* levels. This hypothesis is further substantiated by the finding that *Pax5* inactivation reduces requirements for EBF1 in pro-B cell expansion. The binding of EBF1 and PAX5 to regulatory elements in the human *MYC* gene in a B-ALL cell line indicate that the *EBF1:PAX5:MYC* regulatory loop is conserved and may control both normal and malignant B-cell development.

Key points:

Main point #1: The *Myc* gene is a direct and essential target of EBF1 in early B-lymphocyte development in mice.

Main point #2: EBF1, PAX5 and MYC create a functional loop that control normal pro-B cell expansion in mice.

Introduction.

The formation of lineage restricted progenitor cells during hematopoiesis is under stringent control of transcription factor networks. This is well documented in B-lymphocyte development, where the coordinated action of factors including TCF3, IKZF1, EBF1 and PAX5 control specification as well as lineage restriction [1]. Although the developmental arrest observed in B-cell acute lymphoblastic leukemia (B-ALL) cells establishes a link between development and disease, the finding that several regulators of normal B-cell development are targeted by mutations in malignant cells [2-5] suggests a direct role of transcription factor networks in transformation [6]. These genetic alterations include inactivating mutations in the transcription factors IKZF1, EBF1 and PAX5 [2-5], which are all independently critical for progression of normal B-cell development [6]. Because these transcription factors are essential for normal differentiation, it has been suggested that their reduced functional activities contribute to the developmental arrest observed in B-ALL [3-5]. Support for this idea comes from the finding that re-expression of PAX5 in a leukemia model is sufficient to release the developmental block of the transformed cells [7]. However, leukemia developed more efficiently in mouse models where one allele of *Ebf1* or *Pax5* was inactivated, versus a complete developmental block introduced by homozygous mutation of *Rag1* or *Igμ* [8]. These observations suggest that EBF1 and PAX5 may have more complex roles in the transformation process including control of DNA repair [9] and metabolism [10]. While both PAX5 and IKZF1 act as repressors of metabolism in B-cell progenitors [10], was been reported that EBF1 is critical for cell survival and proliferation in these cells [11-13]. Inactivation of the *Ebf1* gene in pro-B cells results in the rapid loss of progenitor cells *in vivo* that can only be overcome by malignant transformation or, to some extent, by ectopic expression of BCL2L1 or MYB [13]. Together, these

data suggest that EBF1 and PAX5 have distinct and possibly opposing functions in the regulation of cell survival and proliferation in normal B-cell development.

Here, we report that loss of functional EBF1 results in reduced expression of the *Myc* proto-oncogene (*c-Myc*) in B-cell progenitors. Our identification of six distinct EBF1 responsive regulatory elements annotated to the *Myc* gene either by proximity or Proximity Ligated Associated ChIP (PLAC)-seq analysis suggest that *Myc* is a direct target of EBF1 in developing B-cells. Ectopic expression of PAX5 in the absence of functional EBF1 causes partial cell cycle arrest and reduced *Myc* expression supporting the idea that pro-B-cell expansion depends on the opposing effects of EBF1 and PAX5 on the regulation of the *Myc* gene. Our identification of EBF1 and PAX5 binding regions in the human *MYC* locus defines a potential mechanisms for how disruption of this regulatory loop may contribute to malignant conversion of B cell progenitors to cause B-ALL.

Methods:

All animal experiments were performed with the consent of the ethical boards at Linköping and Lund Universities.

For details of experimental procedures please see Supplementary Materials and Methods.

Sequencing data is deposited in GEO as: GSE136238 (Figure S1, Supplementary data sheets) and GSE159957 (Figure 3, 5).

Results:

EBF1 is essential for normal cell expansion in early progenitor cells.

To explore the molecular mechanism by which EBF1 regulates cell survival and proliferation, we utilized a model system based on a 4-Hydroxytamoxifen (4-OHT) responsive EBF1 protein (EBF1-ER) [14] expressed in B-cell progenitors from *Ebf1*$^{-/-}$ mice [15]. This system allows us to dynamically control the function of EBF1 by regulating its nuclear accessibility [14]. Infection of bone marrow (BM) cells from neonatal mice or fetal liver (FL) progenitor cells with retroviruses encoding either a conventional EBF1 or 4-OHT responsive EBF1-ER protein allowed for the formation of CD19^{+} pro-B cells on OP9 stroma cells in the presence of 4-OHT (Figure 1A). Withdrawal of 4-OHT for 72 hours did not result in any significant reduction in live cell recovery of cells rescued by expression of conventional EBF1 (Figure S1A). However, CD19^{+} cells generated by expression of EBF1-ER rapidly responded to removal of 4-OHT by reduced growth and loss of live cells (Figure 1B, S1B). To explore the viability of the cells remaining after 72 hours, we re-plated 10 or 50 live cells on OP9 stroma cells in the presence of 4-OHT. This revealed significantly reduced cloning frequencies of cells pre-incubated in the absence of 4-OHT. Thus, live cells remaining after EBF1 depletion, display an irreversible defect in cellular expansion (Figure S1C). Determination of the cell cycle status of EBF1-ER transduced cells 48 hours after removal of 4-OHT revealed an increased portion of cells in the G0 stage and a relative reduction of cells in G1, S, G2 and M-phase in the absence as compared to the presence of 4-OHT (Figure 1C). Hence, depletion of nuclear EBF1 results in a partial cell cycle arrest with the majority of cells exiting the cell cycle to reside in G0.

The role of EBF1 in pro-B cell expansion was further investigated by transplantation of $CD19^+CD45.2^+$ *Ebf1*$^{-/-}$ cells, rescued by expression of either conventional EBF1 or ER-fused EBF1 by cultivation in 4-OHT, into congenic mice (Figure 1D). While $CD19^+CD45.2^+$ cells expressing conventional EBF1 were detected three weeks after transplantation, few CD45.2 cells were found in the BM of mice transplanted with $CD19^+$ cells rescued *in vitro* by expression of the EBF1-ER protein (Figure 1E-F). These data support the idea that EBF1 is essential for normal pro-B cell expansion [11-13].

To resolve the molecular mechanisms underlying the role of EBF1 in pro/pre-B cell expansion, we used RNA-seq to identify genes with altered expression patterns 72 hours after 4-OHT removal from *Ebf1*$^{-/-}$ EBF1-ER rescued cells. EBF1 expressing cells cultivated either in the presence or absence of 4-OHT were used as a control to identify and exclude drug induced changes in gene expression patterns (Supplementary dataset sheet 1,2, Figure S1D). While mRNA levels from EBF1 target genes such as *Igll1*, *Vpreb3* and *Vpreb2* were reduced upon loss of nuclear EBF1, *Pax5* expression was modestly altered (Figure S1D, Figure 1G, Supplementary dataset sheet 1, 2). We did not detect dramatically reduced levels of the proposed EBF1 targets *Myb* (1.2-fold downregulated) or *Bcl2l1* (1.2-fold upregulated)[13]. Furthermore, we were unable to detect any significant reduction in the levels of phosphorylated STAT5 in the EBF1-ER transduced cells upon removal of 4-OHT (Figure S1E, F). Hence, we do not find support for that the short-term loss of nuclear EBF1 result in collapse of the lineage-specific transcriptional program or dysfunctional IL7 signaling. In contrast, we detected significantly reduced expression of *Myc* by RNA-seq (Figure S1D) as well as RT-Q-PCR (Figure 1G).

MYC has been reported to be essential for normal B-cell development [16,17], and *Myc* expressing tumors have been reported to tolerate loss of EBF1 expression [18]. These observations indicate the existence of a functional interplay between EBF1 and MYC. To investigate a potential functional interaction between MYC and EBF1, we transduced EBF1- or EBF1-ER-rescued *Ebf1*$^{-/-}$ CD19^{+} BM pro-B cells with a bi-cistronic MYC-RFP encoding retroviruses. Enforced expression of MYC had a minor impact on cell recovery in control (MIG), EBF1 or EBF1-ER virus transduced *Ebf1*$^{-/-}$ cells in the presence of 4-OHT (Figure 2A-C). However, while *Ebf1*$^{-/-}$ EBF1-ER cells transduced with the control RFP virus expanded poorly after 4-OHT removal, *Ebf1*$^{-/-}$ EBF1-ER pro-B cells transduced with the MYC encoding virus did not display the same dependency on nuclear EBF1 (Figure 2C). Furthermore, ectopic expression of MYC was sufficient for pro-B cell recovery in the absence of nuclear EBF1 after transplantation of EBF1-ER rescued CD19^{+} cells (Figure 1A) into congenic mice in the absence of 4-OHT treatment (Figure 2D). However, while ectopic expression of MYC allowed for the expansion of CD19^{+} cells *in vivo*, we did not detect generation of IgM^{+} cells in the transplanted mice (Figure 2E). The removal of 4-OHT for 48 hours increased frequencies of apoptotic cells selectively in the EBF1-ER expressing cells, an effect that could not be rescued by ectopic MYC expression (Figure 2F). Hence, ectopic expression of MYC reduced requirements for EBF1 in pro-B cell expansion, but we do not find evidence for that MYC can prevent apoptosis or substitute for EBF1 in B-lineage differentiation.

Because MYC has been suggested to be differentially expressed during the cell cycle [19], we used FACS to determine MYC protein levels in G0, G1, S and G2/M phase pro-B cells. Similar to previous observations [19], MYC protein levels increased progressively from low levels in G0 cells to the highest levels in G2/M phase cells in control pro-B cells as well as in the *Ebf1*$^{-/-}$ cells

expressing the EBF1-ER protein (Figure 2G). The functional inactivation of EBF1 by removal of 4-OHT resulted in an increased of the MYC^{low} G0 fraction relative to the cells cultivated in the presence of 4-OHT. Furthermore, determination of the ratio of MYC protein levels in G0 cells, as compared with those observed in active stages of the cell cycle, revealed that the EBF1-ER expressing G0 cells expressed relatively lower levels of MYC as compared to actively cycling cells in the absence of 4-OHT (Figure 2H). While these data verify that MYC levels are reduced upon inactivation of EBF1, the complex relation between MYC levels and cell cycle progression calls for additional analysis to resolve if *Myc* is a direct target for EBF1 in pro-B cells.

The Myc-gene is a direct target of EBF1 in pro-B cells.

The regulation of the *Myc* gene is highly complex and involve regulatory elements located as far as 1.7 MBp from the coding sequences [20]. Hence, a direct screening of the promoter or proximity annotated distal elements for EBF1 binding sites would not provide an exhaustive identification of EBF1 sites that participate in the regulation of *Myc*. To identify distal regions that interact with the *Myc* promoter in pro-B cells we generated Proximity Ligation Assisted ChIP (PLAC)-seq data from *Wt* and *Ebf1*$^{-/-}$ pro-B cells and carried out a virtual 4C analysis with the *Myc*-promoter as the viewpoint (Figure 3A). This revealed that the major part of the distal interacting elements, including the Blood Enhancer Cluster (BENC)-superenhancer region [20], was located 3´ of the *Myc* gene. Combining PLAC-seq data with ATAC-seq data generated using *Wt* or *Ebf1*$^{-/-}$ pro-B cells [21,22] and analyzing these together with EBF1-ChIP-seq data from 230-238 progenitor B-cells, we identified multiple EBF1 binding elements in the *Myc* locus (Figure 3A). Correlations between the datasets allowed for the identification of one region 5´ of the *Myc* gene (5'E) as well as five putative EBF1 targeted regulatory elements 3´ of the coding gene (Figure 3A, B). One of these

(E1) was located just over 700 kBp from the coding gene while the remaining 4 elements (E2-5) were located between 1.6 and 1.7 Mbp from the TSS within the region defined as harboring the BENC super-enhancer [20]. While E4-5 displayed accessibility, as determined by ATAC-seq analysis, in both *Wt* and *Ebf1*$^{-/-}$ cells, E1-3 accessibility was limited in EBF1 deficient cells indicating that the epigenetic state of these elements depend on EBF1 (Figure 3B). Reanalysis of ChIP- and Cut&Run-seq data from fetal liver pro-B cells (GSE162858), revealed enrichment of acetylated histone H3 lysine K27 (H3K27ac) at the EBF1 bound regions (Figure 3B), indicating that they represent active elements. Further, these regions were enriched for demethylated H3 lysin 4 (H3K4me2) while the levels of the promoter associated tri-methylated Histone H3 lysin 4 (H3K4me3) was low (Figure 3B). These data support the conclusion that elements bound by EBF1 in the *Myc* locus are active enhancers in pro-B cells.

To investigate if these elements act as EBF1 responsive enhancers, we cloned the identified regions into a luciferase reporter vector upstream of a basal *Fos* promoter. The reporter constructs were transfected into Hela cells, lacking expression of endogenous EBF1, together with empty or EBF1 encoding cDNA3 vectors (Figure 3C). Each of the elements responded to the expression of EBF1 by 4-7-fold increases in luciferase activity (Figure 3C) as compared to the 1.6-fold upregulation observed for of the basal Fos promoter (Figure S2A). These data confirm that the *Myc* locus harbors EBF1 responsive regulatory elements.

To investigate whether EBF1 binding sites in these elements are functionally important for normal growth and expansion of pro-B cells we inspected the DNA sequences to identify putative binding sites in all the identified EBF responsive enhancers (Figure 4A). To investigate the ability of these

sites to interact with EBF1 we performed Electrophoretic Mobility Shift Assays (EMSA) (Figure 4B). Binding of *in vitro* translated EBF1 to P^{32} labelled duplex oligonucleotide from the *Cd79a* promoter (Figure S2B) was competed by excess unlabeled putative binding sites from the EBF1 responsive *Myc* enhancers. Binding to the *Cd79a* promoter EBF1 site was efficiently competed by putative binding regions in the *Myc* enhancers (Figure 4B) confirming the presence of EBF1 binding sites in the *Myc* locus.

Having identified EBF1 binding sites, we sought to confirm their function in pro-B cells. To this end we took advantage of a mouse model where the expression of Cas9 is under the regulation of a Tetracycline (Doxycycline) -responsive promoter. These mice were crossed to animals carrying a Doxycycline-dependent transcriptional activator (rTTA) under the control of the broadly active ROSA26 locus. We then designed guide RNAs (gRNAs) targeting several of the EBF1 binding sites as well as the *Myc* coding region. As an additional control we targeted an EBF1 binding site annotated to the *Gfra2* gene, shown redundant for B-cell development [21]. The gRNAs were cloned into lentiviral vector backbones expressing a red-fluorescent marker protein (mCherry). KIT^+ primary BM cells were transduced with the gRNA virus constructs, sorted for expression of mCherry and differentiated *in vitro* into pro-B cells. Before the addition of Doxycyclin, samples of cells were extracted to determine the distribution of gRNAs in the input populations by PCR amplification of viral inserts in genomic DNA (Library 1). After Cas9 induction, the cells were grown for 6 days, the remaining progenitors were collected and the distribution of integrated gRNAs in the genomic DNA of the remaining cells was determined (Library 2). High throughput sequencing of the PCR products allowed us to compare the ratio of guides in the input (Library 1) as compared to the cells present 6 days after induction of Cas9 expression (Library 2). This

revealed a reduced representation of guides 106 and 107, both targeting the same EBF1 binding site in E2 (Figure S2C, 4C). We could also detect a reduced representation of guides targeting the coding region of the *Myc* gene (111 and 112). We noted a modest increase in the relative presence of several guides, likely as a reflection of reduced relative presence of guide 106, 107, 111 and 112. In order to explore the editing efficiency of our gRNAs we amplified the targeted regions in the total population by genomic PCR, sequenced the obtained products and determined mutation rates. Comparing the mutation rates of the target regions to the relative presence of inserted gRNAs suggested efficient editing by all the investigated guides (Figure S2D) indicating that only the EBF1 site in E2 is non-redundant for normal pro-B cell expansion.

To verify the role of the E2 site, we transduced progenitor cells with guide RNA 106 (E2), 107 (E2) (Figure 4C) as well as gRNA 112, targeting the *Myc* gene, and gRNA 81, targeting a putative EBF1 binding site in the *Gfra2* locus. Two days after induction of Cas9 transcription by the addition of Doxycyclin, *Myc* mRNA levels were reduced in the cells transduced with the guides targeting the E2-EBF1 site (sg107, Figure 4D or sg106, Figure S2E) as compared to those expressing sg81. Following the expansion of B-cell progenitors *in vitro* from 24 to 96 hours after the induction of Cas9 expression, we noted the reduced expansion of cells transduced with either guide 106, 107 or 112 as compared to those transduced with the *Gfra2* locus targeting guide 81 (Figure 2E). To determine the targeting efficiency, we extracted DNA from cells harvested 96 hours after CAS9 induction, amplified the targeted region by PCR and sequenced the obtained products. All four guides facilitated mutations in over 70% of the PCR products generated from the target sequences (Figure S2F). Even though mutations could be detected in an area spanning 70bp, the most commonly detected indels, representing 41% (sg106) and 46% (sg107) of the reads

with mutations, involved 5-7 base pairs targeting the EBF1 core binding site (Figure S2G). Performing a motif analysis of the targeted area identified the EBF1 binding site as well as a cryptic E-box, potentially capable to interact with TCF3 or TCF12, and a binding site for TBX1. As the E-box and the TBX1 site were located 3' of the EBF1 core site, these were preferentially targeted by sg106. These data show that mutations in the EBF1 binding region of E2 reduce the expression of *Myc* and pro-B cell expansion. Although the involvement of other factors should not be excluded, these data support the idea that *Myc* is a direct target for EBF1.

EBF1 and PAX5 have opposing roles in the regulation of the Myc-gene.

Next, we wanted to understand the mechanisms by which a progenitor cell develops dependency on EBF1. To this end, we exposed *Ebf1*$^{-/-}$EBF1-ER FL cells to 4-OHT for four or seven days. This relatively short exposure result in a mixture of CD19^{+} and CD19^{-} cells in the cultures. Exposure to 4-OHT for four days impaired the ability of CD19^{-} , and abolished the potential of CD19^{+} progenitor cells, to expand in the absence of 4-OHT in secondary cultures (Figure 5A). This suggests the rapid development of EBF1 dependency in early B-cell progenitors.

Cd19 expression is linked to its transcriptional activation by PAX5, a transcription factor suggested to suppress *Myc* expression [7,23]. Because the *Pax5* gene is a target of EBF1 [24], this suggests that EBF1 and PAX5 function with opposing activities in a regulatory loop controlling *Myc* expression. This idea was supported by that ectopic expression of PAX5 in *Ebf1*$^{-/-}$ cells resulted in reduced cell expansion and formation of CD19^{+} cells 4 days after transduction (Figure 5B, C). The levels of PAX5 protein 24 hours after transduction were comparable to those observed in *Wt* cells arguing against that the observed phenotype was a result of abnormally high PAX5

levels enforced by the retroviral construct (Figure S3). The impact of PAX5 expression on cell proliferation was reflected by the accumulation of cells in G0 (Figure 5D). Determination of the *Myc* expression levels in the surviving PAX5 expressing cells by Q-RT-PCR 72 hours after virus transduction revealed reduced levels compared to those of EBF1 transduced cells (Figure 5E). Analysis of MYC protein levels as a function of cell cycle stage 48 hours after transduction with PAX5- or EBF1-expressing MIG virus revealed a small but significantly increased ratio of MYC protein in G0 versus G1 in the PAX5 transduced cells (Figure 5F). Furthermore, RNA-seq analysis of PAX5 transduced *Ebf1*$^{-/-}$ cells followed by Gene Set Enrichment (GSEA) analysis (Figure 5G) revealed a reduction of the MYC-associated transcriptional program supporting the idea that PAX5 functions as a negative regulator of *Myc* expression in normal B-cell progenitors.

To study the direct role for PAX5 in the induction of EBF1 dependency, we used CRISPR-Cas9-mediated gene targeting to inactivate the *Pax5* gene in CD19^{+} *Ebf1*$^{-/-}$ BM cells expressing either EBF1 or EBF1-ER. FACS analysis of the targeted cells revealed the generation of a CD19^{-} population (Figure 5H) expressing reduced levels of PAX5 (Figure 5I) upon expression of *Pax5* sgRNAs. Assessing the ability of the CD19^{-} cells to expand in the absence of 4-OHT, we noted a significant increase in cell recovery of EBF1-ER rescued cells as compared to cells expressing normal levels of PAX5 (Figure 5J). These data, in combination with the observation that PAX5 binds to regulatory elements in the *Myc* gene (Figure 3A), support that EBF1 and PAX5 create a regulatory loop to regulate cell proliferation in pro-B cells.

Putative regulatory elements in the human MYC locus are targeted by EBF1 and PAX5 in pro-B ALL cells.

To determine whether the human *MYC* gene is targeted by EBF1 and/or PAX5 we took advantage of a combination of ChIP-seq, ATAC-seq and PLAC-seq data [22] to identify regulatory elements interacting with the *MYC* promoter in the human pre-B cell line NALM6. This analysis identified several distal elements displaying ATAC-accessibility and H3K27 acetylation. Several of these elements bound both EBF1 and PAX5 (Figure 6A) revealing that the human *MYC* gene is targeted by both proteins via several putative regulatory elements. Interestingly, this analysis also supported the hypothesis that the *MYC* gene is targeted by IKZF1 and RUNX1 (Figure 6A), which are both frequently mutated and generate fusion proteins in combination with PAX5 and EBF1 in human B-ALL [3-5]. Hence, the regulatory regions of the human *MYC* gene may represent a hub for oncoprotein interaction in B-ALL.

Discussion.

Here, we report that *Myc* is a direct and critical target for EBF1. As MYC has been reported to be essential for B-cell development [16,17], our findings provide a potential explanation for the importance of EBF1 in normal pro-B cell survival and expansion [11-13]. While the functional activity of MYC is regulated at multiple levels including translation, protein stability and interplay with interacting partners [19], our data suggest that EBF1 directly target regulatory elements in the *Myc* locus in non-transformed cells. The regulation of the *MYC* gene has been extensively studied due to the role of this protein in human malignancies [25]. While MYC is broadly expressed, the mouse *Myc* locus is targeted by multiple transcription factors in different tissues, including the lineage restricted transcription factor GATA3 in developing T cells [26]. *Myc* is under the influence of both proximal and distal control elements including the BENC-superenhancer region located approximately 1.7 Mbp from the coding gene [20]. As several of the enhancer elements identified

display reduced ATAC-accessibility in EBF1 deficient cells (Figure 3B), our data support the idea that the BENC-region harbors several independently activated regulatory elements [20]. Of note is that the D-element, located in the BENC-region and shown of importance for B-cell development [20], overlap with the E4 element defined in this report. Due to the lack of suitable gRNAs we did not target this EBF binding site. However, even though the D-deletion spanned approximately 1000 bp [20], these data collectively suggest the presence of two functionally important EBF binding regions in the BENC enhancer. The observation that mutation of any of these elements causes reduced cell growth (Figure 4E) suggest that despite the complexity of this enhancer cluster, there is limited functional redundancy. Hence, while the general idea that transcription regulatory circuits are stable persist [27], *Myc* highlight that the complex interplay between enhancer elements in development [28] may be modulated to fine tune transcriptional programs to create lineage specific regulatory modules.

As the Pax5 gene is a direct target for EBF1 [24], our data suggest that these proteins create a regulatory loop directly involved in the control of pro-B cell expansion. Furthermore, as EBF1 act upstream of PAX5 in B-lymphocyte development, PAX5 mediated repression of cell expansion in the absence of EBF1 would promote an ordered differentiation process. A direct link between expression of a fate determining factor such as EBF1 [11,29-31] and regulation of cell survival and expansion may also be of importance for the preservation of lineage identity. While this would be important in normal development, it is notable that MYC induced B-cell lymphomas display lineage plasticity [32]. Furthermore, cells carrying mutations in the *Ebf1* and/or *Pax5* genes can be converted into T-ALL [33] or even myeloid leukemia [34]. This may be of relevance for leukemia

progression as lineage plasticity is emerging as a potential challenge in lineage targeted treatment of leukemias [34-36].

Our data also provides an insight into how the dosage of lineage-determining factors impacts normal differentiation [37-39]. We here report that a key regulator of cell proliferation (MYC) is subject to both positive and negative regulation by two transcription factors in the same network. Reduced functional dosage of PAX5 could, in this regulatory loop, cause EBF1 to drive *Myc* transcription to higher-than-normal levels (Figure 6B). The complexity of this loop may be extended even further because it has been reported that the mouse *Ebf1* gene contains a MYC responsive enhancer element [16] and that that PAX5 acts as a positive regulator of *N-Myc* [40]. The frequent mutations in PAX5 [2-5] could result in a disruption of the regulatory feedback loop at the *MYC* locus causing EBF1 to super-activate this gene (Figure 6B). It should, however, be noted that the role of EBF1 in a transformed cell appears different from that in normal cells. Requirements for EBF1 in pro-B cells can be circumvented by malignant transformation [13] and it has recently been suggested that EBF1 is a repressor of *Myc* transcription in a mouse model for leukemia [23]. Despite the apparently distinct functions of EBF1 in normal and malignant cells, reanalysis of EBF1 Chip-seq data from normal and transformed cells [23] did not reveal any obvious differences in EBF1 binding at the elements defined in this report. Hence, the mechanism underlying these apparently opposing functions of EBF1 reside is more complex events than alterations in direct DNA binding at these elements.

While data obtained in mouse models should be extrapolated to human disease with great care, our data suggest that the MYC gene may be targeted by several of the key regulators of normal and

malignant B-cell development in humans (Figure 6A). Considering the critical role of MYC in the control of metabolism, cell survival and proliferation in normal and malignant cells [19,41], resolution of the functional interplay between key transcription factors at this locus will likely provide additional insights into the basic mechanisms of neoplastic transformation.

Author contributions: KO, TS, RS, CJ, JTG, MP, JÅ, MS and JU designed conducted and analyzed experiments. SS, JU, CJ and TS contributed to the bioinformatic analysis. JRH and XW contributed essential reagents and analyzed data. MS designed experiments analyzed data and wrote the manuscript draft. All authors contributed to the final version of the manuscript.

Funding: This work was supported by grants from the Swedish Cancer Society (2017-258), the Swedish Childhood Cancer Foundation (2019-0020), the Swedish Research Council (2018-02448), including a Strategic research grant to Stem Therapy, Knut and Alice Wallenberg's Foundation (2014-0089) and a donation from Henry Hallberg (all above to MS) and Lions forskningsfond mot folksjukdomar (to TS). JH is funded by NIH grant R21AI115696 and by the Wendy Siegel Fund for Leukemia and Cancer Research.

Acknowledgments: We are grateful for the technical assistance provided by Liselotte Lenner, Linda Bergström and Maria Malmberg.

Conflict of interest statement: None of the authors has a relevant conflict of interest.

References:

1. Sigvardsson M. Molecular Regulation of Differentiation in Early B-Lymphocyte Development. *Int J Mol Sci*. 2018;19(7).

2. Shah S, Schrader KA, Waanders E, et al. A recurrent germline PAX5 mutation confers susceptibility to pre-B cell acute lymphoblastic leukemia. *Nat Genet*. 2013;45(10):1226-1231.

3. Mullighan CG, Goorha S, Radtke I, et al. Genome-wide analysis of genetic alterations in acute lymphoblastic leukaemia. *Nature*. 2007;446(7137):758-764.

4. Kuiper RP, Schoenmakers EF, van Reijmersdal SV, et al. High-resolution genomic profiling of childhood ALL reveals novel recurrent genetic lesions affecting pathways involved in lymphocyte differentiation and cell cycle progression. *Leukemia*. 2007;21(6):1258-1266.

5. Gu Z, Churchman ML, Roberts KG, et al. PAX5-driven subtypes of B-progenitor acute lymphoblastic leukemia. *Nat Genet*. 2019;51(2):296-307.

6. Somasundaram R, Prasad MA, Ungerback J, Sigvardsson M. Transcription factor networks in B-cell differentiation link development to acute lymphoid leukemia. *Blood*. 2015;126(2):144-152.

7. Liu GJ, Cimmino L, Jude JG, et al. Pax5 loss imposes a reversible differentiation block in B-progenitor acute lymphoblastic leukemia. *Genes Dev*. 2014;28(12):1337-1350.

8. Heltemes-Harris LM, Willette MJ, Ramsey LB, et al. Ebf1 or Pax5 haploinsufficiency synergizes with STAT5 activation to initiate acute lymphoblastic leukemia. *J Exp Med*. 2011;208(6):1135-1149.

9. Prasad MA, Ungerback J, Ahsberg J, et al. Ebf1 heterozygosity results in increased DNA damage in pro-B cells and their synergistic transformation by Pax5 haploinsufficiency. *Blood*. 2015;125(26):4052-4059.

10. Chan LN, Chen Z, Braas D, et al. Metabolic gatekeeper function of B-lymphoid transcription factors. *Nature*. 2017;542(7642):479-483.

11. Nechanitzky R, Akbas D, Scherer S, et al. Transcription factor EBF1 is essential for the maintenance of B cell identity and prevention of alternative fates in committed cells. *Nat Immunol*. 2013;14(8):867-875.

12. Vilagos B, Hoffmann M, Souabni A, et al. Essential role of EBF1 in the generation and function of distinct mature B cell types. *J Exp Med*. 2012;209(4):775-792.

13. Gyory I, Boller S, Nechanitzky R, et al. Transcription factor Ebf1 regulates differentiation stage-specific signaling, proliferation, and survival of B cells. *Genes Dev*. 2012;26(7):668-682.

14. Gao H, Lukin K, Ramirez J, Fields S, Lopez D, Hagman J. Opposing effects of SWI/SNF and Mi-2/NuRD chromatin remodeling complexes on epigenetic reprogramming by EBF and Pax5. *Proc Natl Acad Sci U S A*. 2009;106(27):11258-11263.

15. Lin H, Grosschedl R. Failure of B-cell differentiation in mice lacking the transcription factor EBF. *Nature*. 1995;376(6537):263-267.

16. Vallespinos M, Fernandez D, Rodriguez L, et al. B Lymphocyte commitment program is driven by the proto-oncogene c-Myc. *J Immunol*. 2011;186(12):6726-6736.

17. Habib T, Park H, Tsang M, et al. Myc stimulates B lymphocyte differentiation and amplifies calcium signaling. *J Cell Biol*. 2007;179(4):717-731.

18. Ramirez-Komo JA, Delaney MA, Straign D, et al. Spontaneous loss of B lineage transcription factors leads to pre-B leukemia in Ebf1(+/-)Bcl-xL(Tg) mice. *Oncogenesis*. 2017;6(7):e355.

19. Carroll PA, Freie BW, Mathsyaraja H, Eisenman RN. The MYC transcription factor network: balancing metabolism, proliferation and oncogenesis. *Front Med*. 2018;12(4):412-425.

20. Bahr C, von Paleske L, Uslu VV, et al. A Myc enhancer cluster regulates normal and leukaemic haematopoietic stem cell hierarchies. *Nature*. 2018;553(7689):515-520.

21. Jensen CT, Ahsberg J, Sommarin MNE, et al. Dissection of progenitor compartments resolves developmental trajectories in B-lymphopoiesis. *J Exp Med*. 2018;215(7):1947-1963.

22. Okuyama K, Strid T, Kuruvilla J, et al. PAX5 is part of a functional transcription factor network targeted in lymphoid leukemia. *PLoS Genet*. 2019;15(8):e1008280.

23. Ramamoorthy S, Kometani K, Herman JS, et al. EBF1 and Pax5 safeguard leukemic transformation by limiting IL-7 signaling, Myc expression, and folate metabolism. *Genes Dev*. 2020;34(21-22):1503-1519.

24. Decker T, Pasca di Magliano M, McManus S, et al. Stepwise activation of enhancer and promoter regions of the B cell commitment gene Pax5 in early lymphopoiesis. *Immunity*. 2009;30(4):508-520.

25. Stine ZE, Walton ZE, Altman BJ, Hsieh AL, Dang CV. MYC, Metabolism, and Cancer. *Cancer Discov*. 2015;5(10):1024-1039.

26. Belver L, Yang AY, Albero R, et al. GATA3-Controlled Nucleosome Eviction Drives MYC Enhancer Activity in T-cell Development and Leukemia. *Cancer Discov*. 2019;9(12):1774-1791.

27. Payne JL, Wagner A. Mechanisms of mutational robustness in transcriptional regulation. *Front Genet*. 2015;6:322.

28. Shen Y, Yue F, McCleary DF, et al. A map of the cis-regulatory sequences in the mouse genome. *Nature*. 2012;488(7409):116-120.

29. Zhang Z, Cotta CV, Stephan RP, deGuzman CG, Klug CA. Enforced expression of EBF in hematopoietic stem cells restricts lymphopoiesis to the B cell lineage. *Embo J*. 2003;22(18):4759-4769.

30. Zandi S, Mansson R, Tsapogas P, Zetterblad J, Bryder D, Sigvardsson M. EBF1 is essential for B-lineage priming and establishment of a transcription factor network in common lymphoid progenitors. *J Immunol*. 2008;181(5):3364-3372.

31. Tsapogas P, Zandi S, Ahsberg J, et al. IL-7 mediates Ebf-1-dependent lineage restriction in early lymphoid progenitors. *Blood*. 2011;118(5):1283-1290.

32. Yu D, Allman D, Goldschmidt MH, Atchison ML, Monroe JG, Thomas-Tikhonenko A. Oscillation between B-lymphoid and myeloid lineages in Myc-induced hematopoietic tumors following spontaneous silencing/reactivation of the EBF/Pax5 pathway. *Blood*. 2003;101(5):1950-1955.

33. Somasundaram R, Ahsberg J, Okuyama K, et al. Clonal conversion of B lymphoid leukemia reveals cross-lineage transfer of malignant states. *Genes Dev*. 2016;30(22):2486-2499.

34. Jacoby E, Nguyen SM, Fountaine TJ, et al. CD19 CAR immune pressure induces B-precursor acute lymphoblastic leukaemia lineage switch exposing inherent leukaemic plasticity. *Nat Commun*. 2016;7:12320.

35. Park JH, Geyer MB, Brentjens RJ. CD19-targeted CAR T-cell therapeutics for hematologic malignancies: interpreting clinical outcomes to date. *Blood*. 2016;127(26):3312-3320.

36. Gardner R, Wu D, Cherian S, et al. Acquisition of a CD19-negative myeloid phenotype allows immune escape of MLL-rearranged B-ALL from CD19 CAR-T-cell therapy. *Blood*. 2016;127(20):2406-2410.

37. O'Riordan M, Grosschedl R. Coordinate regulation of B cell differentiation by the transcription factors EBF and E2A. *Immunity*. 1999;11(1):21-31.

38. Ahsberg J, Ungerback J, Strid T, et al. Early B-cell factor 1 regulates the expansion of B-cell progenitors in a dose-dependent manner. *J Biol Chem*. 2013;288(46):33449-33461.

39. Lukin K, Fields S, Guerrettaz L, et al. A dose-dependent role for EBF1 in repressing non-B-cell-specific genes. *Eur J Immunol*. 2011;41(6):1787-1793.

40. Nutt SL, Morrison AM, Dorfler P, Rolink A, Busslinger M. Identification of BSAP (Pax-5) target genes in early B-cell development by loss- and gain-of-function experiments. *Embo J*. 1998;17(8):2319-2333.

41. Muschen M. Metabolic gatekeepers to safeguard against autoimmunity and oncogenic B cell transformation. *Nat Rev Immunol*. 2019;19(5):337-348.

Figure Legends

Figure 1: Loss of functional EBF1 results in reduced levels of *Myc*-transcripts and cell cycle arrest in pro-B cells.

(A) Schematic drawing of the basic experimental layout. Neonatal *Ebf1*$^{-/-}$ BM or *Ebf1*$^{-/-}$ FL were transduced with EBF1-MIG (EBF1) or an EBF1-estrogen receptor fusion protein (EBF1-ER) construct. Cells were then exposed to 4-Hydroxytamoxifen (4-OHT) to allow nuclear translocation of EBF1 in Ebf1-deficient cells carrying the EBF1-ER construct which drives develop into the CD19^{+} stage. 4-OHT was then withdrawn to test the dependency of EBF1 in the generated CD19^{+} cells. (B) Number of live cells of cultured EBF1 or EBF1-ER transduced and 4-OHT treated *Ebf1*$^{-/-}$ BM cell cultures (as in A panel). Cells were either incubated continuously with 4-OHT (+4-OHT) or with 4-OHT withdrawn (-4-OHT) for 48-72 hours as indicated. Mean and SD are shown, n=4, from 4 culture experiments). (C) Cell cycle distributions of the cells in B at 48 hours post 4-OHT withdrawal (mean and SEM are shown, n=6). (D) The experimental protocol used to test the cell autonomous role of EBF1 in pro-B cell survival *in vivo*. *Ebf1*$^{-/-}$ FL cells were transduced to express EBF1 or EBF1-ER and treated with 4-OHT for 14 days. At day 15, 1 million GFP^{+}CD19^{+} cells were transplanted into C57BSJL (CD45.1) sub-lethally irradiated recipients. Donor reconstitution (CD45.2^{+}GFP^{+}) as well as CD19 expression was determined by FACS 3 weeks post transplantation. (E, F) Relative cell counts, from the BM of mice transplanted with either EBF1 or EBF1-ER transduced cells. Mean and SD are shown, EBF1 n=8, EBF1-ER n=11, from 2 independent experiments. Panel (G) display diagrams with Q-RT-PCR data from *in vitro* expanded *Ebf1*$^{-/-}$ fetal liver pro-B control cells (FL) or BM cells from EBF1-deficient mice driven to B-cell progenitor stages with conventional or ER-fused EBF1 protein cultured in the presence or absence

of 4-OHT for 72 hours (mean and SD are shown, n=4-7, from 2 independent experiments). For C, E-G each dot indicates a datapoint and the statistical analysis is based on Student's unpaired t-test. * $p<0.05$, ** $p<0.01$, *** $p<0.001$ and **** $p<0.0001$.

Figure 2: Ectopic expression of MYC rescues pro-B cell expansion in the absence of EBF1. Panel (A-C) display cell recovery from cultures of FL *Ebf1*$^{-/-}$ cells *in vitro* cultivated as described in Figure 1A. Cells were transduced with (A) an empty MIG-GFP (MIGR1) vector, (B) an EBF1-GFP vector (EBF1) or (C) an ER-fused EBF1 protein (EBF1-ER) and serially transduced with an RFP control or a MYC expressing RFP retrovirus. The diagrams display cell recovery when the cells were grown in the presence or absence of 4-OHT for 72 hours (mean and SD are shown, n=6-12, from 3 independent experiments). (D) Recovery of CD45.2^{+}CD19^{+}GFP^{+}RFP^{+} BM cells 3-4 weeks after transplantation of *Ebf1*$^{-/-}$ FL pro-B cells transduced with EBF1-ER and either a control RFP or MYC expressing RFP encoding retrovirus into sub-lethally irradiated CD45.1 mice. Mean and SD are shown, n=4-6 transplanted mice. (E) Representative FACS plot of IgM and CD19 expression on recipient (CD45.1) and donor (CD45.2^{+}GFP^{+}RFP^{+}) cells. (F) Fraction of early (Annexin5^{+}DAPI^{-} (Black bar)) and late (Annexin5^{+}DAPI^{+} (White bar)) apoptotic cells 48 hours after removal of 4-OHT in EBF1 and EBF1-ER expressing *Ebf1*$^{-/-}$ BM cells transduced with either RFP-control or RFP-Myc virus. Mean and SEM are shown (n=3). The statistical analysis is based on comparisons of data from cells grown in the presence or absence of 4-OHT. (G) Histograms displaying overlays of a FACS staining of MYC protein in different stages of the cell cycle and (H) bars depicting the ratios of MYC Median Fluorescent Intensity (MFI) of each stage of the cell cycle compared to G0 48 hours after 4-OHT withdrawal in *Wt* and *Ebf1*$^{-/-}$EBF1-ER BM cells (mean

and SEM are shown, n=6). The statistical analysis is based on Student's unpaired t-test. * $p<0.05$, ** $p<0.01$, *** $p<0.001$ and **** $p<0.0001$.

Figure 3: The mouse *Myc* gene contains multiple EBF1 responsive enhancer elements.

(A) UCSC Genome Browser view of the murine *Myc* locus and its distal interacting regions. The tracks display PAX5 (GSE126375) and EBF1 binding in 230-238 progenitor B cells, ATAC-accessibility (GSE92434), as well as a PLAC-seq derived virtual 4C tracks from *Wt* and *Ebf1*$^{-/-}$ FL derived pro-B-cells. *Myc* transcriptional start site (TSS) ± 2.5kb were used as viewpoint for the virtual 4C analysis. The previously defined BENC-enhancer region [20] is indicated by a dashed square. (B) Zoomed in view of three specific regions in (A) with high PAX5 and EBF1 binding as well as ATAC-accessibility in *Wt* pro-B cells and interaction with the *Myc* promoter. These regions were examined for the presence of histone modifications by reanalysis of ChIP and Cut&Run seq data (GSE162858). The gray lines indicate the regions that are targeted for luciferase reporter activity assays. (C) Relative Firefly/Renilla (Prl0) luciferase activity obtained from reporter constructs where the EBF1 binding regions described in (B) was cloned upstream of a basal *Fos* promoter in the absence (empty cDNA3) or presence of EBF1 in HeLa cells. Each dot represents one transfection and the statistical analysis is based on Student's unpaired t-test. * $p<0.05$, ** $p<0.01$, *** $p<0.001$ and **** $p<0.0001$.

Figure 4: EBF1 directly target an essential binding site in the BENC-enhancer region.

(A) The sequence of known EBF binding sites and six predicted EBF1 binding sites within five putative Myc 3´enhancer elements as well as a potential EBF1 binding site in the 5' region of *Myc*. The core binding site is indicated by a red box (B) Autoradiogram displaying the result of an

EMSA experiment in which the binding of *in vitro* translated EBF1 to a radioactive labelled *Cd79a* promoter-EBF1 site is competed for by the addition of a 200-fold excess of non-labelled putative EBF1 binding sites in *Myc* enhancers or the PAX5 binding site from the *Cd19* promoter. The autoradiogram is representative of two independent experiments. (C) Schematic drawing of the targeting of CRISPR guides 106 and 107 to the EBF1 binding site in *Myc* E2. The DNA sequence of the EBF1 binding motif is depicted in yellow and guides 106 (light brown) and 107 (dark brown) are shown pointing towards a 3' NGG PAM sequence. The scale indicates the genomic location on mouse chromosome 15. (D) *Myc* Q-RT-PCR data from $CD19^+$ iCas9 BM cells transduced with CRISPR guide 81 (control) or 107 (*Myc* E2) and subsequently treated with DOX for 48 hours (mean and SD shown, n=6, from 3 individual samples from different mice). (E) Proliferation per 100 iCas9 $CD19^+$ BM cells at 24, 48 and 96 hours after DOX administration in samples infected with gRNA constructs sg106 and 107 (targeting EBF1 binding site *Myc* E2), sg81 (targeting an EBF1 site linked to the *Gfra2* gene) or sg112 (targeting the coding region of *Myc*). Mean and SD are shown, P * < 0.05, ** < 0.01 (Student's *t* test compared to sg81), from 3 independent samples from different mice.

Figure 5: PAX5 act as a negative regulator of cell proliferation and MYC function in pro-B cells.

(A) Cell recovery 3 days after seeding of 2000 sorted GFP^+CD45^+ *in vitro* expanded FL cells from *Ebf1*$^{-/-}$ mice exposed to nuclear EBF1 by cultivation in 4-OHT for 4 or 7 days before sorting and reseeding in cultures in the absence of 4-OHT (mean and SD are shown, n=5-6, from 2 independent experiments). (B) Total cell recovery and (C) the fraction of $CD19^+$ cells recovered 4 days after seeding 2000 GFP^+ *Ebf1*$^{-/-}$ FL cells transduced with either MIG-control, EBF1 or

PAX5 encoding virus (mean and SD are shown, n=7, from 2 independent experiments). (D) Cell cycle data from *Ebf1*$^{-/-}$ FL cells transduced with MIG-control, EBF1 or PAX5 encoding virus as determined by FACS analysis (mean and SEM are shown, n=3). (E) Q-RT-PCR analysis determining the levels of *Myc* transcripts in live sorted *Wt* FL cells or transduced EBF1 deficient cells as in panel B. Mean and SD are shown, n=4, from 4 samples. (F) The ratio of MYC MFI of each stage of the cell cycle compared to G0 in Ebf1-deficient cells transduced with EBF1 or PAX5 encoding vectors (mean and SEM, n=3). (G) GSEA of genes in HALLMARK_MYC_TARGET_V1 gene set based on RPKM normalized RNA-seq data from *Ebf1*$^{-/-}$ FL cells transduced with a control GFP or PAX5 encoding virus. FDR = False Discovery Rate, NES = Normalized Enrichment Score. (H) Representative histograms of *Ebf1*$^{-/-}$ bone marrow cells rescued to the CD19^{+} pro-B cell stage by transduction with either a conventional or ER-fused EBF1 encoding retrovirus and transduced with a Cas9 encoding virus alone or in combination with a *Pax5* targeting gRNA and (I) MFI values for PAX5 levels as determined by flow cytometry (mean and SD, n=4, from 4 individual samples). (J) Cell recovery after 3 days of *in vitro* culture of EBF1 or EBF1-ER transduced cells expressing Cas9 alone or Cas9 in combination with gRNAs targeted to the *Pax5* gene (gPAX5) (mean and SD, n=4, from 4 individual samples). For A-E, I-J each dot indicates a datapoint and the statistical analysis are based on Student's unpaired t-test. * $p<0.05$, ** $p<0.01$, *** $p<0.001$ and **** $p<0.0001$.

Figure 6: Putative regulatory elements in the human MYC gene is targeted by EBF1 and PAX5 in pro-B ALL cells.

(A) ChIP-seq, ATAC-seq and PLAC-seq tracks for the human *MYC* (*c-MYC*) gene displayed in WashU Epigenome Browser. Data were re-analyzed from [22] (GSE126300). (B) Schematic drawing of a model for regulatory loops controlling *Myc* expression in development.

Figure 1

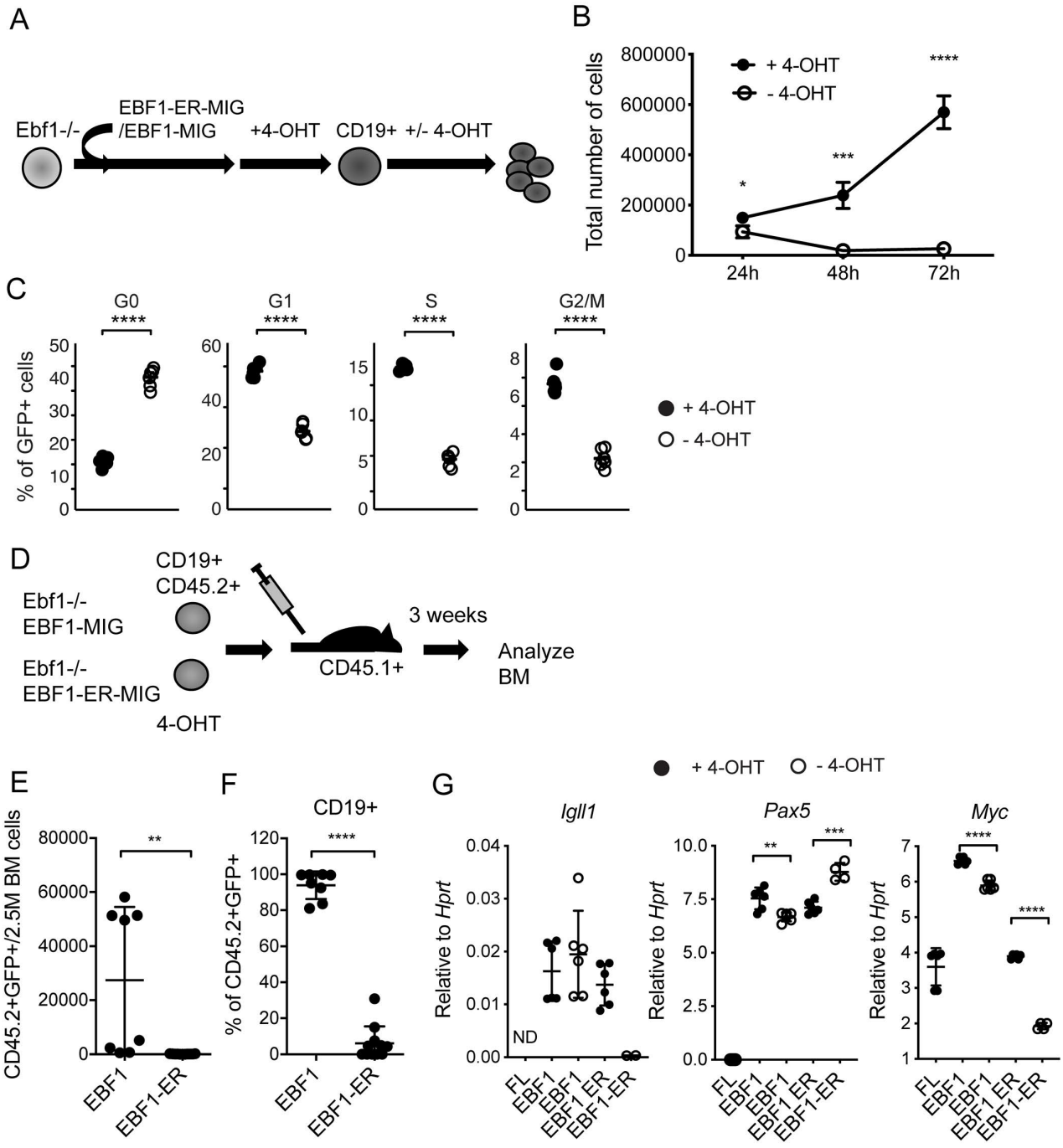
A
Ebf1-/-
EBF1-ER-MIG
/EBF1-MIG
+4-OHT
CD19+ +/- 4-OHT
B
Total number of cells
800000
600000
400000
200000
0
+ 4-OHT
- 4-OHT
*
***
****
24h
48h
72h
C
G0
G1
S
G2/M
****
% of GFP+ cells
+ 4-OHT
- 4-OHT
D
CD19+
CD45.2+
Ebf1-/-
EBF1-MIG
Ebf1-/-
EBF1-ER-MIG
4-OHT
3 weeks
CD45.1+
Analyze
BM
E
CD45.2+GFP+/2.5M BM cells
**
EBF1
EBF1-ER
F
CD19+
% of CD45.2+GFP+
****
EBF1
EBF1-ER
G
+ 4-OHT
- 4-OHT
Igll1
Pax5
Myc
Relative to Hprt
ND
**
***
****
FL
EBF1
EBF1
EBF1 ER
EBF1-ER

Figure 2

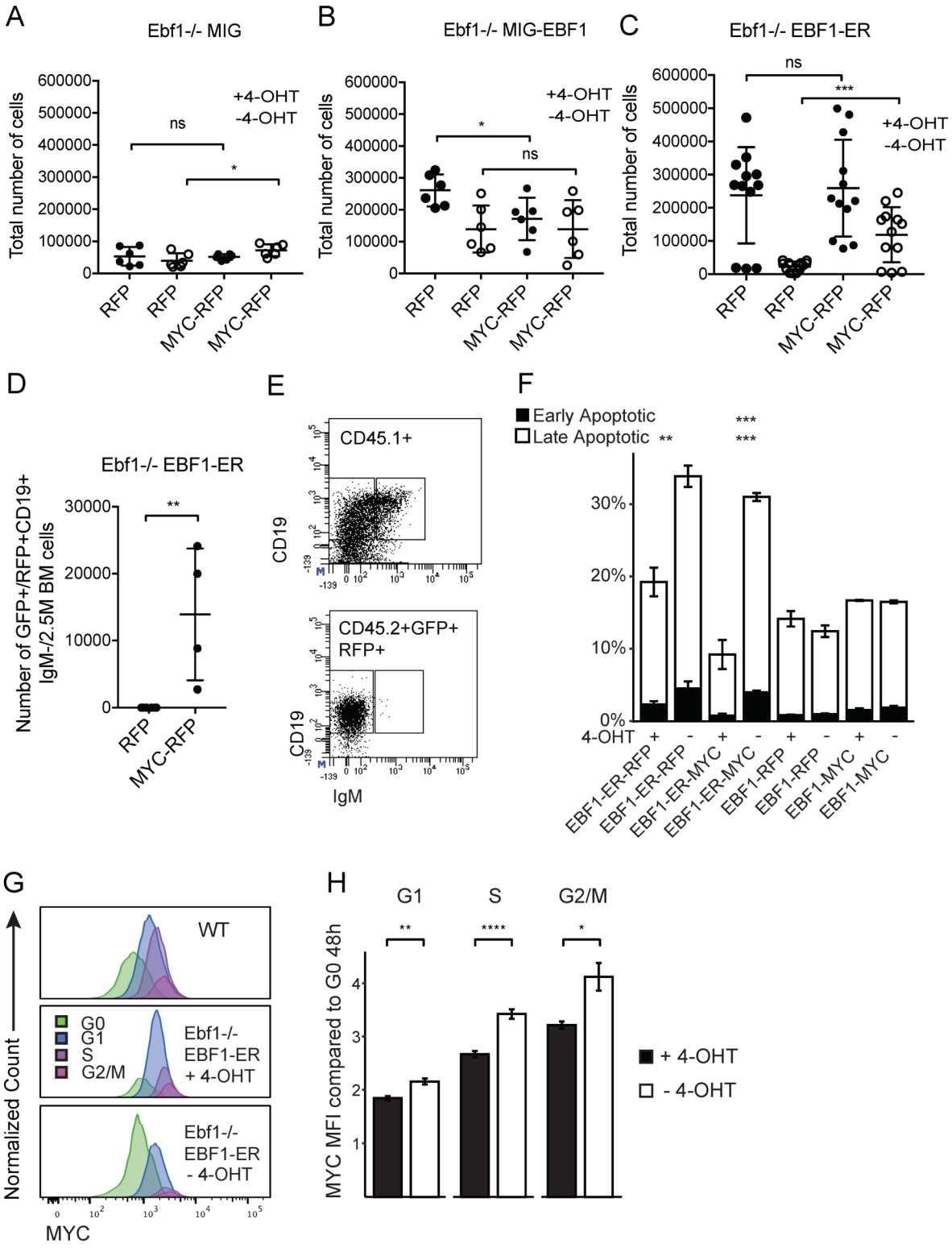
A
Ebf1-/- MIG
Total number of cells
+4-OHT
-4-OHT
ns
*
RFP
RFP
MYC-RFP
MYC-RFP
B
Ebf1-/- MIG-EBF1
C
Ebf1-/- EBF1-ER
D
Ebf1-/- EBF1-ER
Number of GFP+/RFP+CD19+ IgM-/2.5M BM cells
**
E
CD45.1+
CD19
CD45.2+GFP+ RFP+
IgM
F
Early Apoptotic
Late Apoptotic
***
4-OHT
EBF1-ER-RFP
EBF1-ER-MYC
EBF1-RFP
EBF1-MYC
G
WT
G0
G1
S
G2/M
Ebf1-/- EBF1-ER + 4-OHT
Ebf1-/- EBF1-ER - 4-OHT
Normalized Count
MYC
H
G1
S
G2/M
MYC MFI compared to G0 48h
****
+ 4-OHT
- 4-OHT

Figure 3

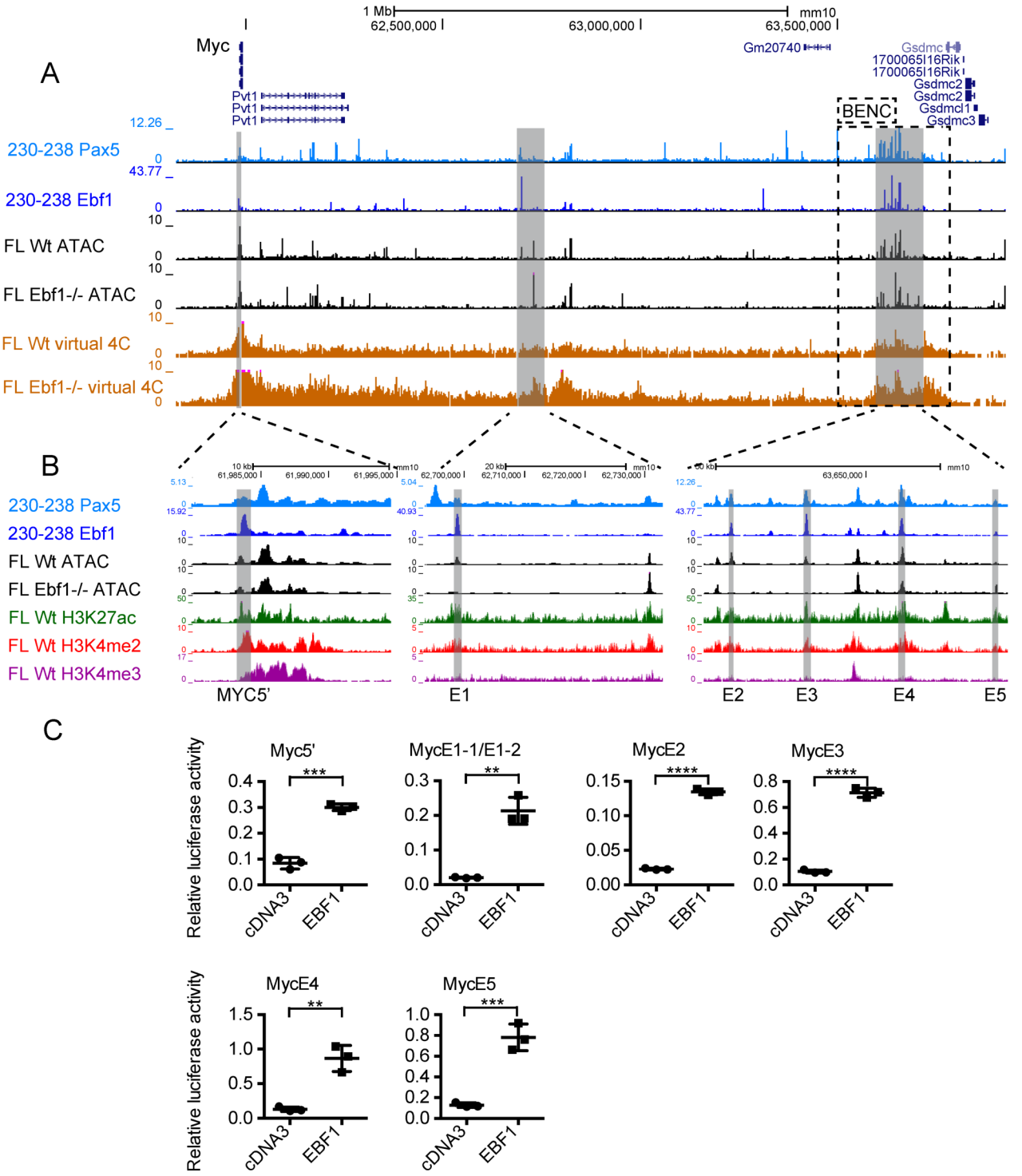
A
1 Mb
62,500,000
63,000,000
63,500,000
mm10
Myc
Gm20740
Gsdmc
1700065I16Rik
1700065I16Rik
Gsdmc2
Gsdmc2
Gsdmc1
Gsdmc3
Pvt1
Pvt1
Pvt1
BENC
230-238 Pax5
230-238 Ebf1
FL Wt ATAC
FL Ebf1-/- ATAC
FL Wt virtual 4C
FL Ebf1-/- virtual 4C
B
230-238 Pax5
230-238 Ebf1
FL Wt ATAC
FL Ebf1-/- ATAC
FL Wt H3K27ac
FL Wt H3K4me2
FL Wt H3K4me3
MYC5'
E1
E2
E3
E4
E5
C
Relative luciferase activity
Myc5'
MycE1-1/E1-2
MycE2
MycE3
MycE4
MycE5
cDNA3
EBF1

Figure 4

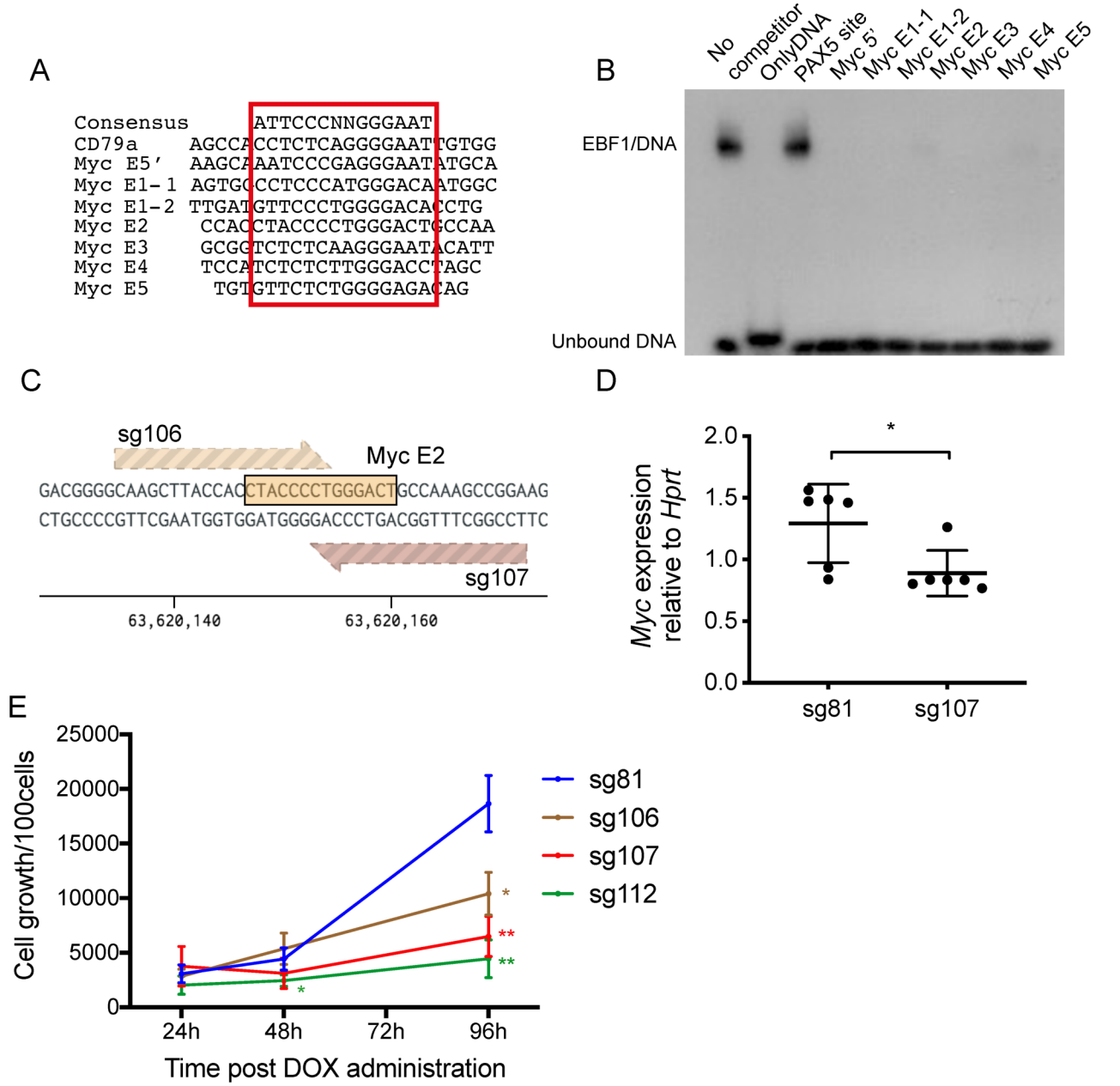
A
Consensus ATTCCCNNGGGAAT
CD79a AGCCACCTCTCAGGGGAATTGTGG
Myc E5' AAGCAAATCCCGAGGGAATATGCA
Myc E1-1 AGTGGCCTCCCATGGGACAATGGC
Myc E1-2 TTGATGTTCCCTGGGGACACCTG
Myc E2 CCACCTACCCCTGGGACTGCCAA
Myc E3 GCGGTCTCTCAAGGGAATACATT
Myc E4 TCCATCTCTCTTGGGACCTAGC
Myc E5 TGTGTTCTCTGGGGAGACAG
B
No competitor
OnlyDNA
PAX5 site
Myc 5'
Myc E1-1
Myc E1-2
Myc E2
Myc E3
Myc E4
Myc E5
EBF1/DNA
Unbound DNA
C
sg106
Myc E2
GACGGGGCAAGCTTACCACCTACCCCTGGGACTGCCAAAGCCGGAAG
CTGCCCCGTTCGAATGGTGGATGGGGACCCTGACGGTTTCGGCCTTC
sg107
63,620,140
63,620,160
D
Myc expression relative to Hprt
2.0
1.5
1.0
0.5
0.0
*
sg81
sg107
E
Cell growth/100cells
25000
20000
15000
10000
5000
0
24h
48h
72h
96h
Time post DOX administration
sg81
sg106
sg107
sg112
*
**
**
*

Figure 5

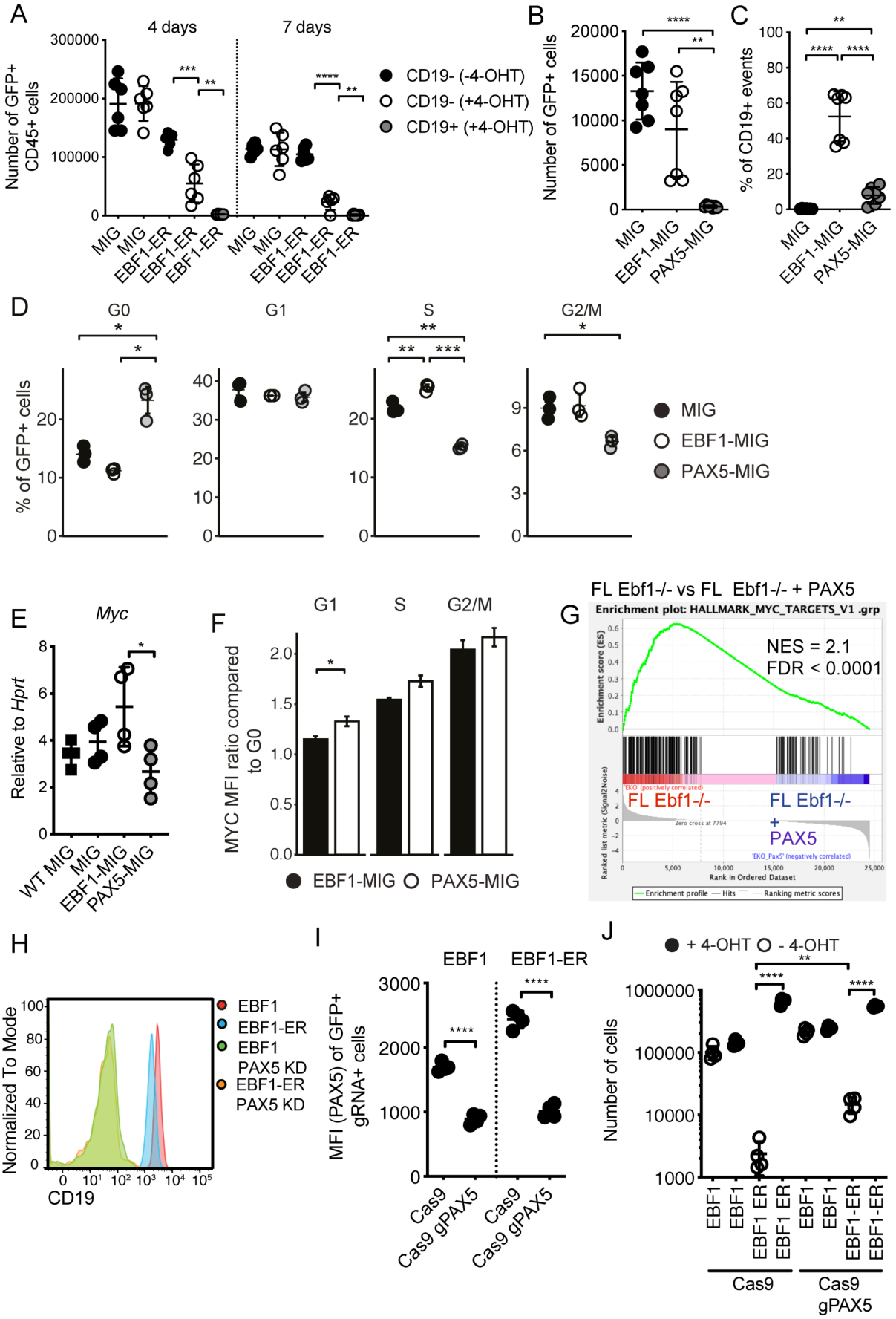
A
4 days
7 days
Number of GFP+ CD45+ cells
CD19- (-4-OHT)
CD19- (+4-OHT)
CD19+ (+4-OHT)
MIG
EBF1-ER
B
Number of GFP+ cells
MIG
EBF1-MIG
PAX5-MIG
C
% of CD19+ events
D
G0
G1
S
G2/M
% of GFP+ cells
MIG
EBF1-MIG
PAX5-MIG
E
Myc
Relative to Hprt
WT MIG
F
G1
S
G2/M
MYC MFI ratio compared to G0
EBF1-MIG
PAX5-MIG
G
FL Ebf1-/- vs FL Ebf1-/- + PAX5
Enrichment plot: HALLMARK_MYC_TARGETS_V1 .grp
NES = 2.1
FDR < 0.0001
Enrichment score (ES)
FL Ebf1-/-
FL Ebf1-/- + PAX5
Rank in Ordered Dataset
Enrichment profile
Hits
Ranking metric scores
H
Normalized To Mode
CD19
EBF1
EBF1-ER
EBF1 PAX5 KD
EBF1-ER PAX5 KD
I
EBF1
EBF1-ER
MFI (PAX5) of GFP+ gRNA+ cells
Cas9
Cas9 gPAX5
J
+ 4-OHT
- 4-OHT
Number of cells
EBF1
EBF1-ER
Cas9
Cas9 gPAX5

Figure 6

A

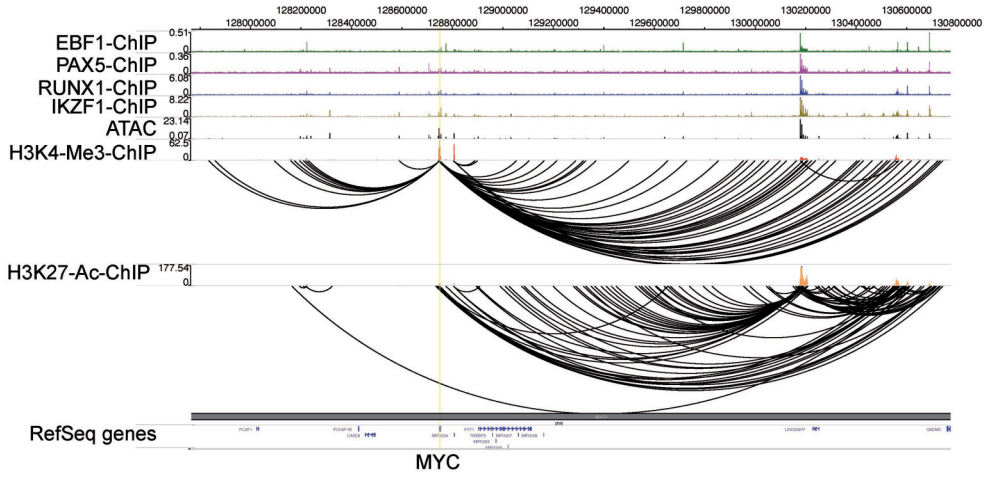
128200000
128600000
129000000
129400000
129800000
130200000
130600000
128000000
128400000
128800000
129200000
129600000
130000000
130400000
130800000
EBF1-ChIP
PAX5-ChIP
RUNX1-ChIP
IKZF1-ChIP
ATAC
H3K4-Me3-ChIP
H3K27-Ac-ChIP
RefSeq genes
MYC

B

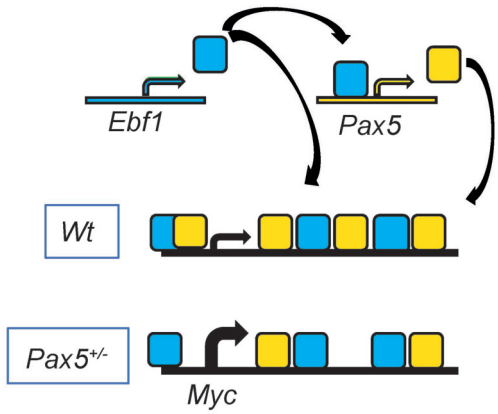
Ebf1
Pax5
Wt
Pax5+/-
Myc